THE JOURNAL OF BIOLOGICAL CHEMISTRY VOL. 286, NO. 50, pp. 43343–43351, December 16, 2011

Structure of Collagen Receptor Integrin α_1I Domain Carrying the Activating Mutation E317A*[S]

Received for publication, May 17, 2011, and in revised form, October 7, 2011 Published, JBC Papers in Press, October 26, 2011, DOI 10.1074/jbc.M111.261909

Matti Lahti[‡1], Eva Bligt[§1], Henri Niskanen[‡], Vimal Parkash[§], Anna-Maria Brandt[§], Johanna Jokinen[‡], Pekka Patrikainen[‡], Jarmo Käpylä[‡], Jyrki Heino[‡], and Tiina A. Salminen[§2]

From the [‡]Department of Biochemistry and Food Chemistry, University of Turku, Turku FI-20014, Finland and the [§]Structural Bioinformatics Laboratory, Department of Biosciences, Åbo Akademi University, Turku FI-20520, Finland

Background: The integrin αI domain undergoes a conformational change during activation.
Results: The crystal structure of an activated αI domain is different from the reported open and closed states.
Conclusion: Our structure mimics the state where the Arg^{287}-Glu^{317} ion pair is just broken during the activation process.
Significance: The activation mechanism of the collagen receptor integrins differs from the other integrins.

We have analyzed the structure and function of the integrin α_1I domain harboring a gain-of-function mutation E317A. To promote protein crystallization, a double variant with an additional C139S mutation was used. In cell adhesion assays, the E317A mutation promoted binding to collagen. Similarly, the double mutation C139S/E317A increased adhesion compared with C139S alone. Furthermore, soluble α_1I C139S/E317A was a higher avidity collagen binder than α_1I C139S, indicating that the double variant represents an activated form. The crystal structure of the activated variant of α_1I was solved at 1.9 Å resolution. The E317A mutation results in the unwinding of the αC helix, but the metal ion has moved toward loop 1, instead of loop 2 in the open α_2I. Furthermore, unlike in the closed αI domains, the metal ion is pentacoordinated and, thus, prepared for ligand binding. Helix 7, which has moved downward in the open α_2I structure, has not changed its position in the activated α_1I variant. During the integrin activation, Glu^{335} on helix 7 binds to the metal ion at the metal ion-dependent adhesion site (MIDAS) of the β_1 subunit. Interestingly, in our cell adhesion assays E317A could activate collagen binding even after mutating Glu^{335}. This indicates that the stabilization of helix 7 into its downward position is not required if the α_1 MIDAS is already open. To conclude, the activated α_1I domain represents a novel conformation of the αI domain, mimicking the structural state where the Arg^{287}-Glu^{317} ion pair has just broken during the integrin activation.

Integrins are bidirectionally signaling, heterodimeric transmembrane receptors, which bind to extracellular ligands, such as matrix proteins, as well as to cytoskeletal and signaling proteins (1). Nine of 18 human integrin α subunits contain a special inserted domain (αI). This domain has a typical dinucleotide binding or Rossman fold, which closely resembles von Willebrand factor A domain (2). Therefore, the inserted domains can also be called as integrin αA domains. In the integrin αI domain a central hydrophobic β sheet is surrounded by seven amphipathic α helices. The ligand binds to a Mg^{2+} ion in the metal ion-dependent adhesion site (MIDAS)[3] and interacts with certain surrounding amino acid residues (2).

The human αI domain integrins can be divided into two subcategories: collagen receptor and leukocyte integrins. Collagen receptor integrins ($\alpha_1\beta_1$, $\alpha_2\beta_1$, $\alpha_{10}\beta_1$, and $\alpha_{11}\beta_1$) participate in platelet adhesion, proliferation of mesenchymal stem cells, development of cartilage, and innate and acquired immunity (3). Leukocyte integrins ($\alpha_D\beta_2$, $\alpha_E\beta_7$, $\alpha_L\beta_2$, $\alpha_M\beta_2$, and $\alpha_X\beta_2$) recognize plasma proteins, *e.g.* component C3b in the complement system, and counterreceptors on other cells, such as intercellular cell adhesion molecules (ICAMs) (4). These integrins regulate, for example, leukocyte adhesion to endothelium and homing (5). The general structure of the αI domains in these two subcategories is similar. Collagen binding αI domain, however, contains an additional helix, called the αC helix, which is important for ligand binding (2, 6, 7).

Integrin $\alpha_1\beta_1$ is a collagen receptor expressed mainly on mesenchymal cells (8). Based on the analysis of the α_1-deficient mice and the *in vivo* experiments utilizing specific function-blocking antibodies, the biological tasks of integrin $\alpha_1\beta_1$ include the regulation of immune response (9, 10), mesenchymal stem cell proliferation (11, 12), and matrix turnover (13, 14). Basement membrane collagen IV has been suggested to be the main ligand for integrin $\alpha_1\beta_1$ (15, 16). Integrin $\alpha_1\beta_1$ can, however, recognize many other collagen subtypes, such as fibril-forming collagens, fibril-associated collagens with interrupted triple helices, transmembrane collagens, and network-

* This work was supported by the Academy of Finland; the Sigrid Jusélius Foundation; the Cancer Society of Finland; the Cancer Society of Southwestern Finland; the Tor, Joe, and Pentti Borgs Foundation; the Finnish Cultural Foundation; the Varsinais-Suomi Regional fund; the Turku graduate school of Biomedical Sciences; and the National Doctoral Programme in Informational and Structural Biology.

[S] The on-line version of this article (available at http://www.jbc.org) contains supplemental Fig. S1.

The atomic coordinates and structure factors (code 4A0Q) have been deposited in the Protein Data Bank, Research Collaboratory for Structural Bioinformatics, Rutgers University, New Brunswick, NJ (http://www.rcsb.org/).

[1] Both authors contributed equally to this work.
[2] To whom correspondence should be addressed. Tel.: 358-40-5151201; E-mail: tiina.salminen@abo.fi.

[3] The abbreviations used are: MIDAS, metal ion-dependent adhesion site; ICAM, intercellular cell adhesion molecule; MEM, minimum essential medium; PDB, Protein Data Bank.

forming collagens (for review, see Ref. 3). Integrin $\alpha_1\beta_1$ can also bind to distinct laminin subtypes and semaphorin 7A (17).

In $\alpha_1\beta_1$, as in all αI domain integrins, the ligand binding takes place at the MIDAS of the αI domain. The atomic structures of the α_L, α_M, α_X, α_1 (human and rat) and α_2 I domains have been solved (6, 18–23). The structure of the closed form of α_1I and α_2I (PDB code 1AOX) (6) are almost identical, as their structural superimposition gives a root mean square deviation of 0.62 Å for 177 C_α atoms. In the active site, the metal ion and the surrounding residues occupy identical positions in both structures, and the αC helix is stabilized by the Arg^{287}-Glu^{317} (α_1I numbering) ion pair interaction as well. The structures of the α_LI domain in complex with ICAM-1 or ICAM-5 (24, 25), as well as α_2I in complex with a collagenous GFOGER peptide have also been solved (26). Ligand binding opens the αI domain by triggering large conformational changes in the αC helix and helix 7 and some spatial adjustments in the MIDAS. The αC helix in the α_2I domain unwinds and swings away from the vicinity of the MIDAS. Helix 7 moves significantly downward, allowing a specific glutamate to bind to the MIDAS of the I domain of the β subunit. Glu^{310} in αL, Glu^{320} in αM, and Glu^{336} in α2 are supposed to stabilize helix 7 in the open conformation and mediate structural changes between integrin α and β subunits (24, 27–29). These conformational modifications can also lead to the separation of the integrin leg parts and promote cell signaling.

Here, we have characterized the collagen binding properties of an activated variant of the α_1I domain, harboring a gain-of-function mutation E317A (30). To promote protein yield, solubility, and crystallization, a double variant with an additional C139S mutation was used. In cell adhesion assays E317A mutation promoted binding to collagen. Similarly, double mutation C139S/E317A increased adhesion compared with C139S alone. Furthermore, E317A could increase cell adhesion even after the connection between α_1I and β_1 subunits had been prevented by E335A mutation. The solved 1.9 Å crystal structure of the activated variant of α_1I has a novel conformation, which is different from the previously reported "open" and "closed" αI domains.

EXPERIMENTAL PROCEDURES

Materials—Rat collagen I was purchased from Sigma-Aldrich, and collagen IV from mouse Engelbreth-Holm-Swarm tumor was from BD Biosciences. Bovine serum albumin (BSA) was from Bovogen Biologicals.

Mutagenesis of Human Integrin α_1 and Its α_1I Domain—The α_1I domain including the amino acids (^{138}ECS-LEATA^{338}) was previously cloned into the pGEX-4T vector (Amersham Biosciences) (23, 31). The full-length α_1 human integrin constructed in pcDNA3.1/Z-2 plasmid (Invitrogen) was a kind gift from Dr. Pauli Ollikka (Biotie Therapies Corp.). The point mutations (C139S, E317A, C139S/E317A, E335A, and E335A/E317A) to both full-length α_1 and α_1I were carried out using a QuikChange site-directed mutagenesis kit (Stratagene). All clones were sequenced to ensure that undesired mutations were not introduced during PCR. Plasmid constructs (pcDNA3.1/Z-2/α_1 and its variants) were transfected into Chinese hamster ovary (CHO) cells (American Type Culture Collection, ATCC) as described previously for α_2 (29). FuGENE6 (Roche Applied Science) was used for transfection in CHO cells. Two days after transfection, transformants were selected with 150 μg/ml Zeocin (Invitrogen) in α-MEM. After 2 weeks, positive cells were stained with integrin α_1 antibody (purified anti-human CD49a, SR-84; BD Pharmingen) and anti-mouse IgG FITC antibody (Santa Cruz Biotechnology) and collected as mixed populations using FACSVantage SE flow cytometry (BD Biosciences).

Cell Adhesion Assays—Attachment and spreading of chimeric $\alpha_1\beta_1$ (human α_1, hamster β_1) expressing CHO cells was tested with xCELLigence real-time cell analyzer (RTCA; Roche Applied Science). This technology measures impedance at the bottom of a microtiter plate well and allows estimating the progression of cell attachment and spreading. E-plates 96 (Roche Applied Science) were coated either with collagens I, IV (5 μg/cm^2/well; 16.4 μg/ml) or BSA (0.1%) in Dulbecco's phosphate-buffered saline (PBS; Sigma) overnight at 4 °C. Before coating collagen I was diluted in acetic acid (0.1 M) to keep it in monomeric, triple helical form. Coated wells were washed with PBS and blocked with BSA for 1 h (0.1% in PBS, 5% CO_2, 37 °C). After blocking, BSA was removed, and α-MEM (without FCS) was added to the wells. The background signal was measured, and 40,000 cells/well were added. BSA was used as the negative control, and its signal was measured for each cell line with three parallel wells (data not shown). The Mann-Whitney *U* test with SPSS software (version 16.0; IBM) was used for statistical analysis of the data collected at the 1-h time point. Cell adhesion was followed for 2 h at 37 °C (5% CO_2). The cells used in these experiments were collected from almost confluent culture plates. Trypsin-EDTA solution (Sigma) was used to remove the cells from the plate, and trypsin inhibitor (Sigma) was added. The cells were spun down at 500 × *g* for 5 min at 37 °C, and the pellet was resuspended using α-MEM medium without FCS.

Protein Expression and Purification—For solid phase binding assays, protein expression and purification was performed as described earlier (30). Briefly, glutathione *S*-transferase (GST) fusion proteins were expressed in *Escherichia coli* BL21 Tuner™ (Novagen). For crystallization of α_1I C139S/E317A, the protein was produced using 100 ml of overnight culture to inoculate 15 liters of LB_{AMP}-medium and cultured in Bioengineering fermentor (Bioengineering AG) at 37 °C until the $A_{600\ nm}$ reached 0.5–0.6. To induce expression of the protein, isopropyl β-D-1-thiogalactopyranoside was added to a final concentration of 0.4 mM. Protein production was continued at room temperature for 6 h and at 10 °C overnight. The cells were harvested by centrifugation, and the GST fusion protein was purified as described earlier (30). GST was removed by thrombin digestion (GE Healthcare). 100 units of thrombin were added every 2nd h for 8 h. GST was separated from the α_1I domain by GST-affinity chromatography using disposable columns (Bio-Rad). Protein was further purified by gel filtration chromatography (HiLoad™26/60 Superdex™200 preparation grade; GE Healthcare) using Äkta FPLC. The purified protein was concentrated using Centriprep centrifugal filter device (Millipore) followed by buffer exchange to 40 mM Tris (hydroxymethyl) aminomethane, pH 7.2, 2 mM $MgCl_2$, and 20% glycerol. Finally, the protein was concentrated using Centricon centrifugal filter device (Millipore) to 23–28 mg/ml. The purity of the protein

TABLE 1
Statistics of the structure determination of the activated α_1I C139S/E317A

Data collection	
Beamline	ID14-1 (ESRF, Grenoble)
Space group	P3
Unit cell dimensions (Å, °)	$a = b = 95.5$, $c = 37.8$; $\alpha = \beta = 90$, $\gamma = 120$
Resolution limits (Å)	47.86–1.90 (2.05–1.90)
No. of observed reflections	172,075 (34,565)
No. of unique reflections	30,076 (6,099)
Wavelength (Å)	0.93
Matthews coefficient (Å^3/Da)	2.26
Solvent content (%)	45.5
Molecules/assymetric unit	2
Completeness (%)	99.3 (99.2)
Redundancy	5.7 (5.7)
R_{sym} (%)	6.1 (45.6)
R_{meas} (%)	6.7 (50.2)
R_{merge}-F (%)	8.7 (41.9)
Average I/σ	20.1 (4.1)
Wilson B-factor	23.6
Refinement statistics	
PDB code	4A0Q
Resolution range (Å)	20.00–1.90
Reflections	28,552
R_{cryst} (%)	18.6
R_{free} (%)	22.9
No. of amino acids	374
No. of water molecules	185
Average B-factor for all atoms (Å^2)	28.3
Ramachandran plot (%)	
Most favored	97.5
Additional allowed	2.2
Disallowed regions	0.3

was checked by electrophoresis on 8–25% gradient polyacrylamide gels in the presence of 0.55% SDS using the Phast System (Amersham Biosciences).

Solid Phase Binding Assays—Binding assays were carried out as described previously (30, 32). 96-well plates were coated overnight at 4 °C with either collagens I, IV (5 μg/cm^2/well) or BSA (3.75%) that was used for blocking the wells. GST fusion α_1I domains were allowed to bind for 1 h in the presence of 2 mM $MgCl_2$ in Delfia® assay buffer (PerkinElmer Life Sciences). Wells were washed three times, and the signal was detected with Delfia® europium-labeled anti-GST antibody (PerkinElmer Life Sciences). Label was dissociated with Delfia® enhancement solution (PerkinElmer Life Sciences), and the signal was determined using a time-resolved fluorescence spectrophotometer (Victor3 multilabel counter; PerkinElmer Life Sciences). Estimates for the dissociation constants (K_d) were obtained using the following equation: measured binding = maximal binding/(1 + K_d/[αI]).

Crystallization and Data Collection—Initial screening for crystallization conditions was done with the sparse matrix screen JCSG+ Suite (Qiagen) using the hanging drop vapor diffusion method. The crystals were grown at 8 °C by mixing 1 μl of 26 mg/ml protein solution in 40 mM Tris, pH 7.4, 2 mM $MgCl_2$, and 20% glycerol with 1 μl of the well solution, which contained 1.6 M trisodium citrate. In a week, the crystals grew to the final size of 0.3 × 0.1 × 0.1 mm^3. The crystal was picked directly from the crystallization plate and flash frozen with liquid nitrogen. The crystal diffracted to 1.9 Å, and the data were collected on ADSC Quantum Q210 detector installed on beamline ID 14-1 at the European Synchrotron Radiation Facility (ESRF, France). The data were integrated and scaled in space group P3 using the XDS and XSCALE programs (33).

Structure Determination, Model Building, and Refinement—The solvent content of the crystal was 45.5%, with two chains in the asymmetric unit (Table 1). The structure of α_1I C139S/E317A was determined by molecular replacement using the program Molrep (34, 35). We searched for two α_1I domains using closed α_1I (PDB code 1PT6) (23) as a search model. 5% of the reflections (1,428) were randomly selected for R_{free} calculation, and the remaining data (28,552) were used in refinement (Table 1). Using Refmac5 (36), the initial R-factor after rigid body refinement was 27.6% (R_{free} = 26.6). ARP/wARP Solvent (37) was used for the addition of water molecules. The Refmac5 refinement was followed by manual model building in COOT (38). Iterative model building and refinement gave a final model with R-factor 18.6% (R_{free} = 22.9). The electron density quality was good throughout both chains except for the weak electron density of the residues 286–291 in chain B and the total lack of electron density for the residues 286–290 in chain A. The final model was validated using Molprobity (39). All the structural figures were made with PyMOL (40).

RESULTS

Activation of Integrin $\alpha_1\beta_1$ by α_1 E317A Mutation Leads to High Avidity Cell Adhesion to Collagens I and IV—In our previous studies, we have identified α_1I E317A as a gain-of-function mutation, which improves collagen binding considerably (30). To investigate the integrin activation further, we used CHO cells transfected to express wild-type (WT) α_1 and mutant integrins (α_1 E317A, α_1 C139S, α_1 C139S/E317A). Flow cytometry experiments confirmed comparable expression levels for the variant and WT α_1 integrins (supplemental Fig. S1). The effect of integrin mutations on cell adhesion was analyzed using the xCELLigence instrument. This technology measures

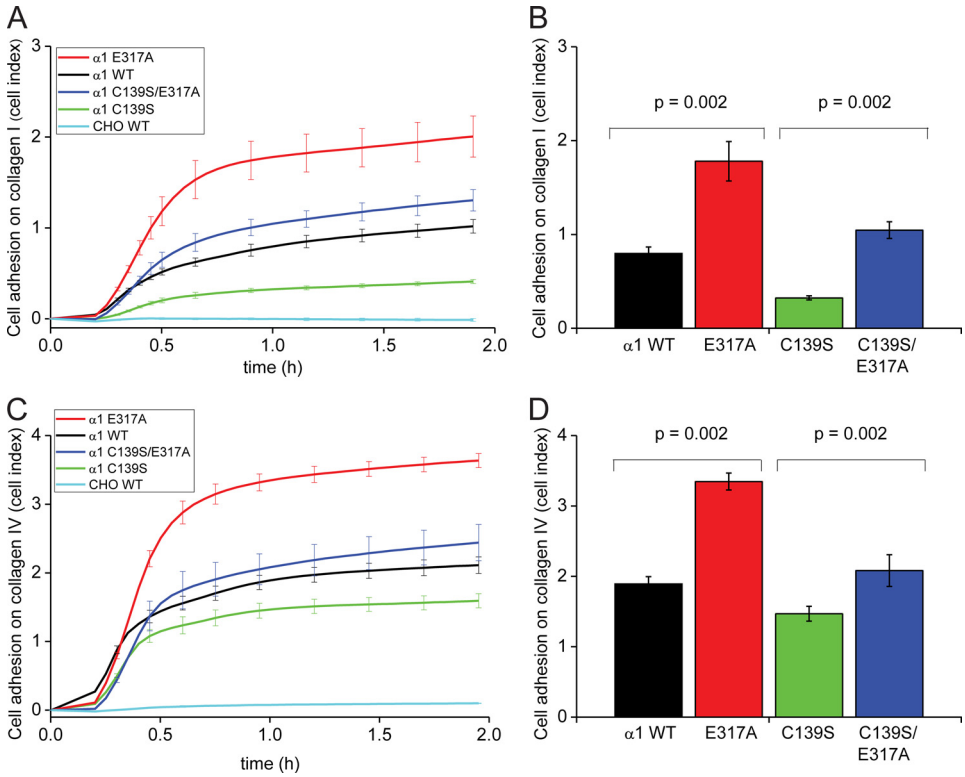

FIGURE 1. **Activation of integrin $\alpha_1\beta_1$ leads to high avidity cell adhesion to collagens I and IV.** *A* and *C*, cell adhesion was measured on collagen I (*A*) and collagen IV (*C*) for both high affinity variants (E317A, C139S/E317A) of human α_1 in CHO cells using xCELLigence real-time cell analyzer. The 96-well E-plates were coated either with collagens I or IV in PBS. Coated wells were washed with PBS and blocked with BSA. BSA was removed and α-MEM (without FCS) was added to the wells. Background signal was measured, and 40,000 cells/well were added. Six replicates were used for each collagen samples. *B* and *D*, data at the 1-h time point were taken from the corresponding data sets, *A* and *C*, respectively. The *p* values showed in the panels were estimated according to the Mann-Whitney *U* test.

impedance at the bottom of a microtiter plate well and allows following the progression of cell attachment and spreading. The E317A mutation in α_1 caused significant increase in cell adhesion to both collagen I and IV compared with WT α_1 ($p = 0.002$, Mann-Whitney *U* test, cell adhesion to collagen I or collagen IV at 1-h time point). Similarly, cell adhesion studies with α_1 C139S/E317A indicated that the double variant is a better binder of collagens than α_1 C139S ($p = 0.002$, Mann-Whitney *U* test, cell adhesion to collagen I or collagen IV at 1-h time point) (Fig. 1). Even though C139S alone reduces adhesion, E317A mutation could significantly activate cell adhesion even in the presence of C139S. Importantly, WT and variant α_1 integrins showed better adhesion to collagen IV compared with collagen I, suggesting that the mutations had not changed the ligand specificity.

As a Soluble, Recombinant Protein the C139S/E317A Variant of the α_1I Domain Shows an Increased Avidity to Collagen Compared with the α_1I C139S—The collagen binding properties of the soluble, recombinant α_1I C139S and α_1I C139S/E317A variants were studied in a solid phase binding assay. The double variant containing the activating E317A mutation (α_1I C139S/E317A) bound to both collagen I and IV significantly better than α_1I C139S (Fig. 2). Furthermore, based on K_d values, α_1I C139S binds to collagens I and IV with similar avidity, whereas α_1I C139S/E317A binds to collagen IV more tightly than to collagen I. The results suggest that E317A activates the α_1I domain even in the presence of the C139S mutation. Because of its higher avidity, we have named α_1I C139S/E317A as an activated form of α_1I.

X-ray Structure of Activated α_1I C139S/E317A—The structure of the double variant C139S/E317A of the ligand-free α_1I domain was solved by molecular replacement using the closed conformation of α_1I (PDB code 1PT6) (23) as a search model. We refined the structure using Refmac5 (36) to a final *R*-factor of 18.6% (R_{free} = 22.9%). Statistics for the data processing and structural refinement are summarized in Table 1. The asymmetric unit in the crystal contains two molecules, which are identical, and their structural superimposition gives a root mean square deviation of 0.06 Å for 177 C_α atoms. Each chain comprises residues 142–333, 185 water molecules, and a Mg^{2+} bound at the MIDAS. The region of residues 138–141 in the N terminus of both chains is disordered, so the mutation C139S is not visible in the structure. The electron density map was good throughout the structure except for the loop region 286–290 (Fig. 3). The residues 286–290 in the loop region in chain A could not be built because of the lack of electron density, and only the main chain atoms are built for chain B (Fig. 3*B*). In the following, we therefore discuss only chain B. The core structure is similar to the closed form of the WT α_1I with a central hydrophobic β sheet sandwiched by six amphipathic α helices.

Activating E317A Mutation Caused Significant Conformational Changes in αC Helix—The αC helix (residues 283–287) stabilized by the Arg^{287}-Glu^{317} ion pair interaction plays important role in collagen binding (7). The αC helix unwinds

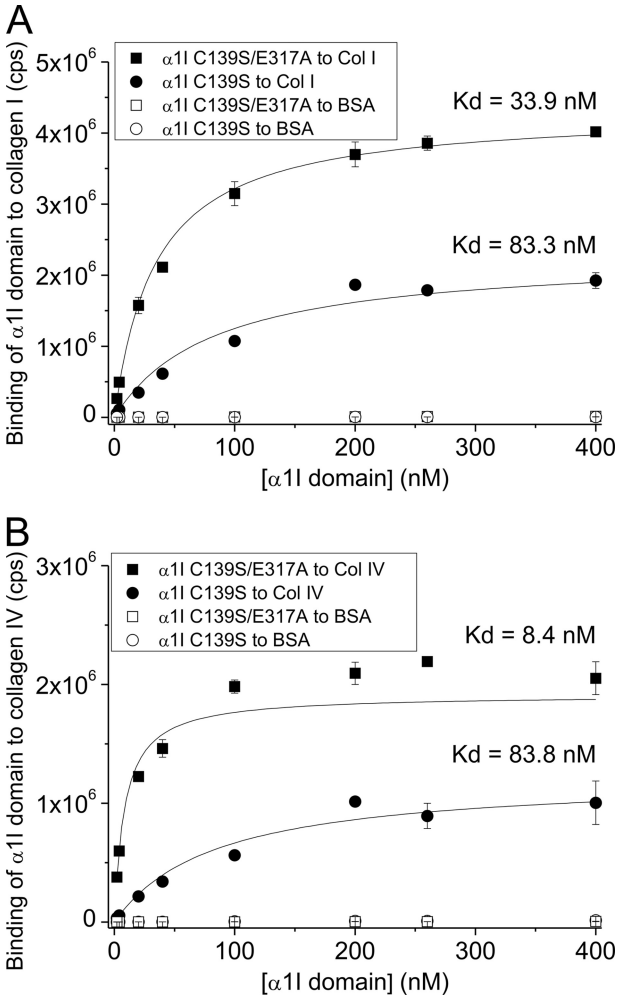

FIGURE 2. **The gain-of-function variant of α_1I C139S/E317A variant has increased collagen I and collagen IV avidity compared with α_1I C139S.** Binding of the α_1I C139S and α_1I C139S/E317A variants to collagen I (*A*) and collagen IV (*B*) was studied in a solid phase binding assay. 96-well plates were coated either with collagen I, IV, or BSA in PBS. BSA served as a negative control and was also used for blocking the wells. GST fusion α_1I domains were allowed to bind for 1 h in the presence of 2 mM $MgCl_2$ in Delfia® assay buffer. Wells were washed, and the signal was detected with Delfia® europium-labeled anti-GST antibody. Label was dissociated with Delfia® enhancement solution, and the signal was determined using a time-resolved fluorescence spectrophotometer. Each sample was measured with three parallel wells. Estimates for the dissociation constants were obtained using an equation: measured binding = maximal binding/(1 + K_d/[αI]).

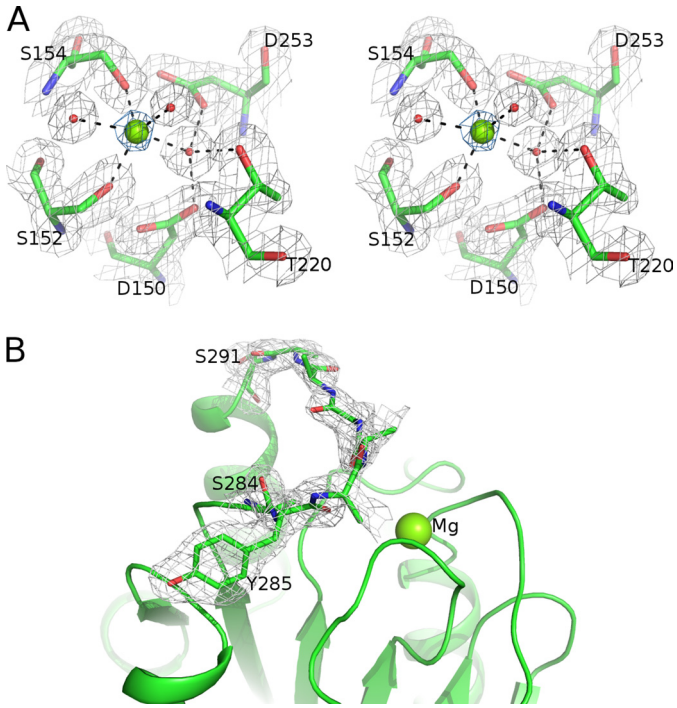

FIGURE 3. **$2F_o - F_c$ electron density maps in the MIDAS and the αC helix of the monomer B of the α_1I C139S/E317A.** *A*, stereo representation of the MIDAS. The map for the Mg^{2+} ion is contoured at 3.0 σ (shown in *blue*), and the map for the other residues is contoured at 1.2 σ (shown in *gray*). *B*, unwound αC helix, residues 284–291. Residues 286–290 in this region are disordered, and only the main chain is visible. The electron density map is contoured at 1.0 σ. Residues are presented as *sticks*: carbon, *green*; oxygen, *red*; nitrogen, *blue*; and the Mg^{2+} ion is shown as a *green sphere*.

when collagen binding to the MIDAS disrupts Arg^{287}-Glu^{317} interaction (26). Compared with the closed form of α_1I (Fig. 4*A*, green), where Tyr^{285} restricts the ligand binding to the MIDAS, in our activated C139S/E317A structure (Fig. 4*A*, *salmon*) the αC helix unwinds and Tyr^{285} is moved away from the MIDAS. As a result of this movement, the active site opens. This is to our knowledge the first structure of the α_1I domain with the unwound αC helix in the absence of collagen.

MIDAS of Activated α_1I—In the MIDAS of the integrin αI domain residues from three loops (L1, L2, and L3) surround the metal ion in the active site and coordinate the metal directly or indirectly (Fig. 5). Compared with the hexacoordination of the metal in previously published α_1I and α_2I structures, the metal ion in our activated α_1I structure forms a pentacoordinated complex (see below), where Ser^{152} and Ser^{154} from L1 and three water molecules coordinate the metal through their hydroxyl oxygen (Fig. 5*B*).

Activated α_1I C139S/E317A Shows Differences in MIDAS, αC Helix, Helix 6, and Helix 7 Compared with Open α_2I Structure—The core structure of our activated α_1I is very similar to the open α_2I. However, it is different from the open α_2I with respect to the MIDAS, the αC helix, helix 6, and helix 7. The metal coordination in our activated α_1I structure is slightly different from both closed and open αI (Fig. 5, *A*–*C*). The direct binding of Ser^{152} and Ser^{154} (α_1I numbering) to the metal is conserved in all the structures. In the activated α_1I, the metal moves (2.2 Å) toward L1 with respect to its position in the closed α_1I (Fig. 5*B*). This is similar but not identical to the metal ion movement between the open and closed α_2I, where the metal moves 2.6 Å toward L2 (26). Because of the metal ion movement toward L1 in the activated α_1I, the conserved threonine (Thr^{220}) on L2 interacts with the metal via another water molecule (Fig. 5*B*) unlike in the open α_2I where Thr^{221} binds directly to the metal (Fig. 5*C*). Similar to the open α_2I structure, Asp^{253} in the activated α_1I makes a water-mediated contact to the metal (Fig. 5*E*).

As in the open α_2I structure, the αC helix of the activated double variant has unwound to a loop structure. Although the residues near the MIDAS are mostly conserved, the residues Ser^{284} and Tyr^{285} in the αC helix of α_1I correspond to Tyr^{285} and Leu^{286} in α_2I, respectively (Fig. 5*D*). Despite these differences in the amino acid sequences, the tyrosine residue is turned away from the MIDAS in both open α_2I and activated

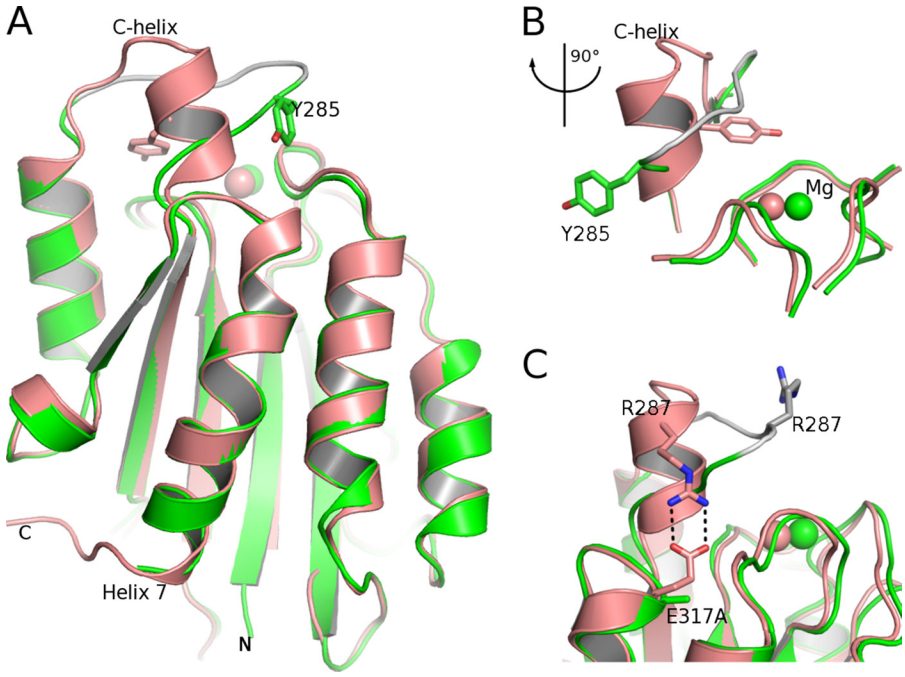

FIGURE 4. **Superposition of the activated and the closed forms of the α_1I domain.** *A*, overall view of the α_1I C139S/E317A superimposed on the closed form of the integrin α_1I domain. The closed form is shown in *salmon*, and the activated conformation is in *green*. The Mg^{2+} ions are shown as *spheres* in respective colors. The αC helix is unwound to a flexible loop in the activated structure. The region of the loop, residues 286–290, is presented in *gray*. The position of helix 7 is identical in both structures. *B*, close-up view of the MIDAS. Tyr^{285} points away from the MIDAS in the activated structure whereas it covers the MIDAS in the closed form. In the activated α_1I structure, the position of the Mg^{2+} ion has shifted by 2.2 Å. *C*, E317A mutation breaking the ion pair Arg^{287}-Glu^{317} in the activated α_1I structure.

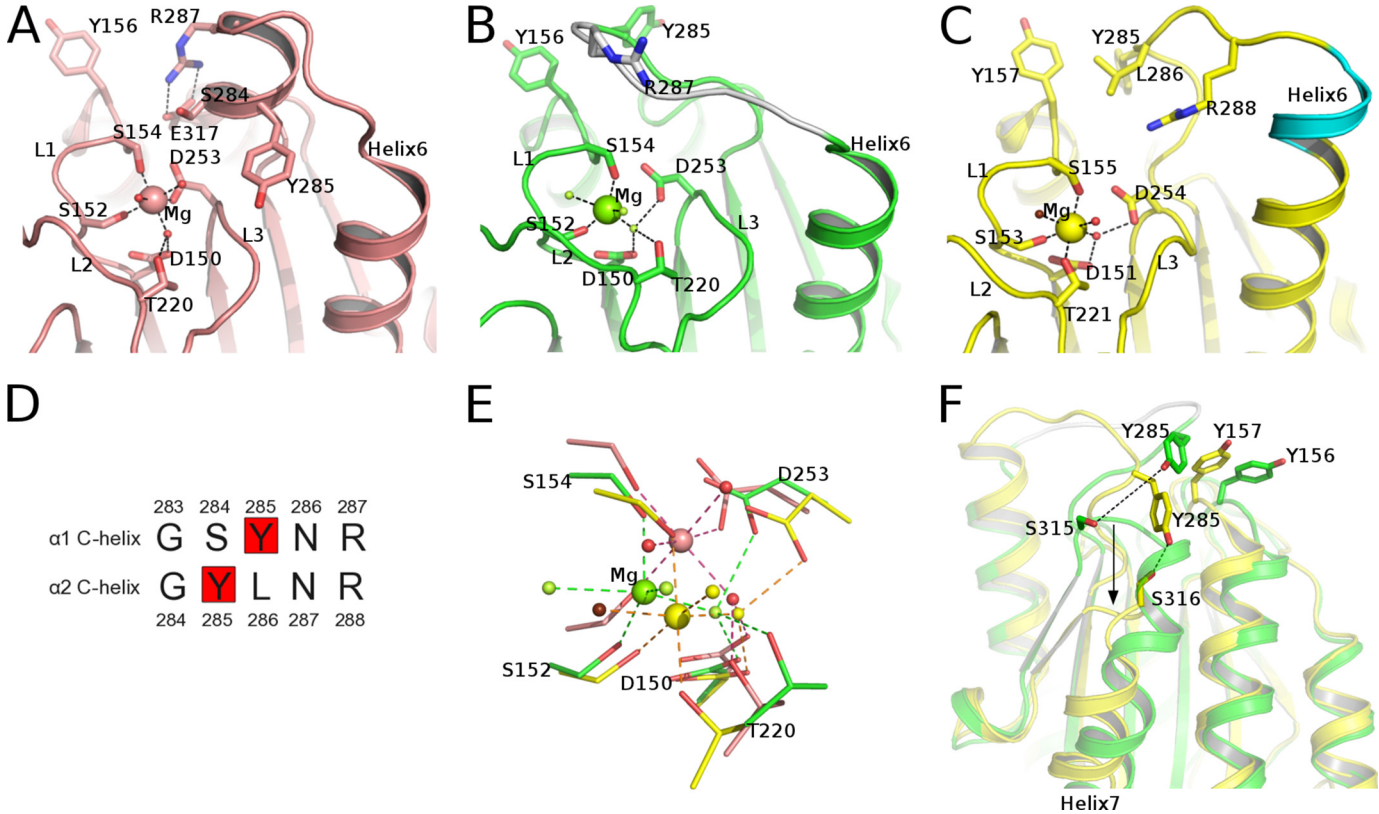

FIGURE 5. **Comparison of the closed, activated, and open form of αI structures.** A, α_1I in the closed conformation (*salmon*, PDB code 1PT6). *B*, activated conformation of α_1I C139S/E317A (*green*). *C*, open α_2I (*yellow*, PDB code 1DZI). The *brown sphere* represents Glu^{11} from the bound ligand. The extra turn on top of helix 6 resulting from the unwinding of the αC helix is shown in *cyan*. *D*, residues corresponding to Ser^{284} and Tyr^{285} in α_1I (*salmon, panel A*) are Tyr^{285} and Leu^{286} in α_2I (*yellow, panel C*). *E*, close-up view of the comparison of the MIDAS of the three structures. *F*, side view of the open α_2I (*yellow*) and the activated α_1I C139S/E317A (*green*) to see differences in helix 7. The *arrow* points to the difference in the loop structures before helix 7.

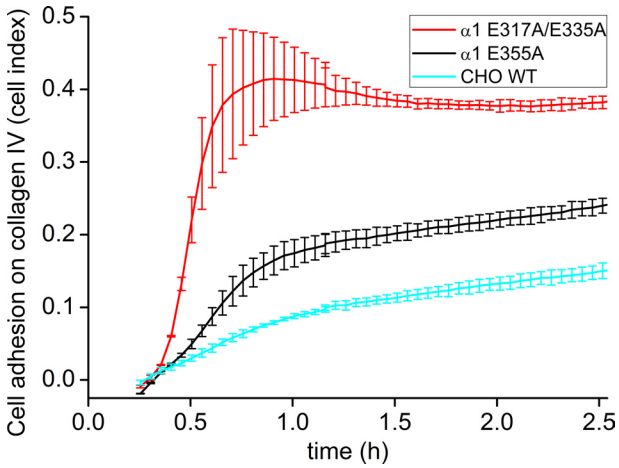

FIGURE 6. **Activation of integrin α_1I does not require the link between α_1I and β_1I domains in the presence of the activating mutation E317A.** Cell adhesion was measured on collagen IV for variants E335A and E317A/E335A of human α1 in CHO cells using xCELLigence real-time cell analyzer. The 96-well plates were coated with collagen IV in PBS. Coated wells were washed with PBS and blocked with BSA. BSA was removed, and α-MEM (without FCS) was added to the wells. Background signal was measured, and 40,000 cells/well were added. Three replicates were used for each sample.

α_1I structures; Tyr^{285} in α_1I points toward Ser^{315}, and Tyr^{285} in α_2I is hydrogen-bonded to Ser^{316} (Fig. 5*F*). Unlike in the open ligand-bound α_2I structure, the uncoiling of the αC helix does not lead to an extra turnover helix 6 (Fig. 5, *B* and *C*). Furthermore, helix 7 in the collagen-bound open α_2I structure moves downward but does not show such a change in the activated α_1I structure (Fig. 5*F*).

Link between α_1I and β_1I Domains Is Not Required for E317A-related α_1I Activation—Previous research has indicated that helix 7 in the αI domain is linked to the β subunit by a specific glutamate residue that acts as an "intrinsic ligand" for the MIDAS in the βI domain. Glu^{310} in α_L and Glu^{320} in α_M are supposed to mediate conformational changes between the two integrin subunits (24, 27, 28). Similarly, mutation of an equivalent residue Glu^{336} in α_2 subunit inactivates $\alpha_2\beta_1$ integrin (29). Because in our novel activated α_1I domain structure the activation was not associated with a concomitant movement of helix 7, we decided to study whether also at the cellular level $\alpha_1\beta_1$ activation could take place without the relocation of helix 7. In this purpose we introduced mutation E335A alone and in combination with E317A into the α_1 subunit, expressed the variant integrins in CHO cells, and measured their binding to collagen IV using xCELLigence technology (Fig. 6). At the 1-h time point E335A mutation decreased cell adhesion about 10-fold compared with α1 WT transfected CHO cells (Fig. 1), whereas the second mutation E317A partially reversed the effect resulting in 2.5-fold increase (Fig. 6). Thus, E317A-related structural changes in the α_1I domain do not require the relocation or stabilization of helix 7 in a Glu^{335}-dependent manner.

DISCUSSION

The mutation E318A in α_2I activates collagen and laminin binding (30, 41). We have previously introduced the equivalent E317A mutation to α_1I and shown its activating character (30). To get the first three-dimensional structure of an activated collagen receptor α_1I without a ligand, we had to introduce an additional mutation, namely C139S, to increase the protein yield and solubility. Equivalent cysteine to serine mutation has been used to decrease the aggregation of α_MI domain (42). We used both solid phase binding assay and cell adhesion assay to confirm that the mutant α_1I C139S/E317A still represents an activated αI domain. Kinetically, α_1I C139S/E317A resembles α_1I WT, binding more tightly to collagen IV than to collagen I. Interestingly, C139S mutation alone decreased both the αI domain binding to collagen and cell adhesion. We also know based on our earlier experiments that the short α_1I and α_2I domain constructs lacking this particular cysteine show weaker binding to collagens.[4] In the $\alpha_X\beta_2$ heterodimer (PDB code 3K6S) (43), the corresponding cysteine links the α_XI domain to the β propeller domain in the α_X subunit by forming a disulfide bond with a cysteine residue in the β propeller. The loss of this stabilizing disulfide would explain the decreased activity of the $\alpha_1\beta_1$ heterodimer harboring the α_1 C139S mutation. However, the stabilization mechanism of C139 in the recombinant α_1I domain remains unknown.

Collagen binding to the αI domain initiates the loss of the Arg^{287}-Glu^{317} ion pair interaction (Fig. 4*C*), which leads to the unwinding of the αC helix. We originally predicted that the loss of the salt bridge in the α_1I E317A variant would trigger large conformational changes similar to those seen in the collagen-like peptide bound α_2I (26), including the downward movement of helix 7 (30). However, our activated mutant structure revealed unexpected and interesting mechanism for the αI domain activation without any change in the position of helix 7. Even though the activation of α_1I domain is due to the gain-of-function mutation and, therefore, not physiological, the unveiled atomic structure can be used to explain the activation mechanism.

Enhanced ligand binding of the α_1I C139S/E317A variant could be explained by the fact that Tyr^{285}, which covers the MIDAS in the closed form (23), has moved aside and unwinds the αC helix making the MIDAS more accessible for the ligand. Tyr^{285} in α_1I is not conserved and does not correspond to Tyr^{285} in α_2I (Fig. 5*D*); however, it seems to take the role of Tyr^{285} in α_2I (Fig. 5*F*). This could result in differences between the open forms of α_1I and α_2I, because the αC helix might not be long enough in α_1I to reorganize an additional turn on helix 6. This would also mean that the open form of α_1I is different from the homology model of the open α_1I (23, 30), which was predicted based on the ligand-bound α_2I structure (26). It seems reasonable to speculate that the change in the metal ion coordination (from penta- to hexacoordinated) upon ligand binding to the activated mutant α_1I would induce the change of the activated form to a fully open form of α_1I where helix 7 is in the downward position. Because the opening of the αC helix does not have an effect on helix 7, we propose that interaction with collagen or a collagen like peptide is necessary to push helix 7 into the position required for interaction with the MIDAS of the βI domain. Recently, the structure of the α_LI domain in complex with its ligand ICAM-5 showed the unusual allosteric mobility of helix 7 (25).

[4] M. Lahti, E. Bligt, H. Niskanen, V. Parkash, A.-M. Brandt, J. Jokinen, P. Patrikainen, J. Käpylä, J. Heino, and T. A. Salminen, unpublished data.

Previous studies have proposed that the open αI domain conformation is also possible without a ligand and represents an activated integrin conformation. Gain-of-function mutations can be used to open the αI domain structure and experimentally mimic the activated αI domains. The activated αI domains, which enhance helix 7 movement, are reported for α_XI I314G (44), α_MI F302W (45), and α_MI I316R and I316G (42). Also, cysteine substitutions that stabilize open conformations via disulfide bonds can be used to activate integrin αI domains: α_2I G172C/L322C (46), α_LI K287C/K294C, α_LI E284C/E301C (24), α_MI C128A/D132C/K315C (47), α_MI Q163C/Q309C, α_MI D294C/Q311C (48). In another study, stable open conformation of α_MI was computationally designed, and numerous mutations were introduced to obtain the desired conformations (49). Based on simulations of molecular dynamics and energy minimization α_LI and α_MI, unlike α_1I and α_2I, are considered to also have an intermediate form (50). The structure of the activated α_1I variant solved in this study is also clearly different from the intermediate form of α_LI (24). In the activated α_1I domain, all of the structural changes had taken place close to the MIDAS, whereas in the intermediate-affinity I domain structure helix 7 was partially shifted down, and the MIDAS was closed.

The functional stage of all integrins is strictly regulated (51, 52). In general, a bent integrin conformation is considered to be unable to bind to large ligands. Integrin preactivation has been considered to take place after the inside-out signals have induced the binding of cytoplasmic proteins, *e.g.* talin or kindlin, to the cytoplasmic domain of the integrin β subunit (53). The movement of integrin legs apart may then lead to integrin extension and a conformational change in the βI domain. A specific glutamate residue (*e.g.* Glu^{310} in α_L and Glu^{320} in α_M) in αI domain acts as a link to the MIDAS in βI domain and may transfer the conformational change from the β subunit to the αI domain. In this integrin activation model, helix 7 is first pulled down, which then opens and activates the αI domain structure (51, 52). The activation of integrin $\alpha_X\beta_2$ requires both extension and an open headpiece (54). However, the collagen receptor αI domain integrins may behave in a different manner. We have shown that the nonactivated $\alpha_2\beta_1$ integrin can effectively bind to a large size ligand, namely human echovirus-1 (EV-1) (55). Furthermore, the collagen receptor integrin αI domains purified as recombinant proteins can recognize ligands with relatively good avidity even in the closed conformation (7, 16, 30, 41, 56). We have used mutagenesis to address the question, whether the stabilization of the downward-moved position of helix 7 by β_1I is required for the activation of α_1I domain. In $\alpha_1\beta_1$ integrin, the residue in the α_1I domain that acts as an intrinsic ligand for the β_1I domain is Glu^{335}. Mutating Glu^{335} to alanine in $\alpha_1\beta_1$-expressing CHO cells leads to weaker cell adhesion on collagen IV. Interestingly, the double variant of α_1 containing E335A and the activating mutation E317A restored adhesion of the CHO cells, which indicates that the Glu^{335}-mediated binding to β_1I is not necessary for the activation of $\alpha_1\beta_1$ integrin (Fig. 6).

Integrin functions can also be regulated by lateral interactions with other membrane proteins, *e.g.* syndecan family heparan sulfate proteoglycans (57), tetraspanins, and urokinase-type plasminogen activator receptor (58). There seem to be direct or indirect interactions between integrins and these proteins, but very little is known about the structural basis of the mechanism that they use in integrin regulation. It is possible to speculate that the integrin conformation can be modified by other membrane proteins, which would *e.g.* induce the breakage of the Arg^{287}-Glu^{317} salt bridge and consequently unwind the αC helix. It remains to be seen, however, whether the novel α_1I domain conformation represents this kind of activation mechanism.

To conclude, we have solved to our knowledge the first atomic structure of an activated collagen receptor α_1I domain. The conformational changes explain the enhanced ligand binding, but are clearly different compared with the previously published closed/intermediate/open αI domain structures. Our data indicate that the activated α_1I domain may also differ from the ligand-bound, open α_1I domain.

Acknowledgments—We thank Alex Vogel for assistance with crystallization and Prof. Mark Johnson for the excellent computing facilities at Åbo Akademi University. We acknowledge the European Synchrotron Radiation Facility for provision of synchrotron radiation resources. Beam time was made available under the European Union Improving Human Potential Programme (Access to Research Infrastructures) at the ESRF under contract No. HPRI-CT-1999–00022. Use of Biocenter Finland infrastructure at Åbo Akademi (bioinformatics, structural biology and translational activities) is acknowledged.

REFERENCES

1. Hynes, R. O. (2002) *Cell* **110,** 673–687
2. Lee, J. O., Bankston, L. A., Arnaout, M. A., and Liddington, R. C. (1995) *Structure* **3,** 1333–1340
3. Heino, J. (2007) *BioEssays* **29,** 1001–1010
4. Evans, R., Patzak, I., Svensson, L., De Filippo, K., Jones, K., McDowall, A., and Hogg, N. (2009) *J. Cell Sci.* **122,** 215–225
5. McEver, R. P., and Zhu, C. (2010) *Annu. Rev. Cell Dev. Biol.* **26,** 363–396
6. Emsley, J., King, S. L., Bergelson, J. M., and Liddington, R. C. (1997) *J. Biol. Chem.* **272,** 28512–28517
7. Käpylä, J., Ivaska, J., Riikonen, R., Nykvist, P., Pentikäinen, O., Johnson, M., and Heino, J. (2000) *J. Biol. Chem.* **275,** 3348–3354
8. Voigt, S., Gossrau, R., Baum, O., Löster, K., Hofmann, W., and Reutter, W. (1995) *Histochem. J.* **27,** 123–132
9. Fiorucci, S., Mencarelli, A., Palazzetti, B., Sprague, A. G., Distrutti, E., Morelli, A., Novobrantseva, T. I., Cirino, G., Koteliansky, V. E., and de Fougerolles, A. R. (2002) *Immunity* **17,** 769–780
10. Ray, S. J., Franki, S. N., Pierce, R. H., Dimitrova, S., Koteliansky, V., Sprague, A. G., Doherty, P. C., de Fougerolles, A. R., and Topham, D. J. (2004) *Immunity* **20,** 167–179
11. Pozzi, A., Wary, K. K., Giancotti, F. G., and Gardner, H. A. (1998) *J. Cell Biol.* **142,** 587–594
12. Ekholm, E., Hankenson, K. D., Uusitalo, H., Hiltunen, A., Gardner, H., Heino, J., and Penttinen, R. (2002) *Am. J. Pathol.* **160,** 1779–1785
13. Gardner, H., Broberg, A., Pozzi, A., Laato, M., and Heino, J. (1999) *J. Cell Sci.* **112,** 263–272
14. Chen, X., Moeckel, G., Morrow, J. D., Cosgrove, D., Harris, R. C., Fogo, A. B., Zent, R., and Pozzi, A. (2004) *Am. J. Pathol.* **165,** 617–630
15. Kern, A., Eble, J., Golbik, R., and Kühn, K. (1993) *Eur. J. Biochem.* **215,** 151–159
16. Tulla, M., Pentikäinen, O. T., Viitasalo, T., Käpylä, J., Impola, U., Nykvist, P., Nissinen, L., Johnson, M. S., and Heino, J. (2001) *J. Biol. Chem.* **276,** 48206–48212

17. Suzuki, K., Okuno, T., Yamamoto, M., Pasterkamp, R. J., Takegahara, N., Takamatsu, H., Kitao, T., Takagi, J., Rennert, P. D., Kolodkin, A. L., Kumanogoh, A., and Kikutani, H. (2007) *Nature* **446,** 680–684
18. Lee, J. O., Rieu, P., Arnaout, M. A., and Liddington, R. (1995) *Cell* **80,** 631–638
19. Qu, A., and Leahy, D. J. (1995) *Proc. Natl. Acad. Sci. U.S.A.* **92,** 10277–10281
20. Nolte, M., Pepinsky, R. B., Venyaminov, S. Yu, Koteliansky, V., Gotwals, P. J., and Karpusas, M. (1999) *FEBS Lett.* **452,** 379–385
21. Salminen, T. A., Nymalm, Y., Kankare, J., Käpylä, J., Heino, J., and Johnson, M. S. (1999) *Acta Crystallogr. D Biol. Crystallogr.* **55,** 1365–1367
22. Rich, R. L., Deivanayagam, C. C., Owens, R. T., Carson, M., Höök, A., Moore, D., Symersky, J., Yang, V. W., Narayana, S.V., and Höök, M. (1999) *J. Biol. Chem.* **274,** 24906–24913
23. Nymalm, Y., Puranen, J. S., Nyholm, T. K., Käpylä, J., Kirdon, H., Pentikäinen, O.T., Airenne, T. T., Heino, J., Slotte, J. P., Johnson, M. S., and Salminen, T. A. (2004) *J. Biol. Chem.* **279,** 7962–7970
24. Shimaoka, M., Xiao, T., Liu, J. H., Yang, Y., Dong, Y., Jun, C. D., McCormack, A., Zhang, R., Joachimiak, A., Takagi, J., Wang, J. H., and Springer, T. A. (2003) *Cell* **112,** 99–111
25. Zhang, H., Casasnovas, J. M., Jin, M., Liu, J. H., Gahmberg, C. G., Springer, T. A., and Wang, J. H. (2008) *Mol. Cell* **31,** 432–437
26. Emsley, J., Knight, C. G., Farndale, R. W., Barnes, M. J., and Liddington R. C. (2000) *Cell* **101,** 47–56
27. Alonso, J. L., Essafi, M., Xiong, J. P., Stehle, T., and Arnaout, M. A. (2002) *Curr. Biol.* **12,** R340–342
28. Yang, W., Shimaoka, M., Salas, A., Takagi, J., and Springer, T. A. (2004) *Proc. Natl. Acad. Sci. U.S.A.* **101,** 2906–2911
29. Connors, W. L., Jokinen, J., White, D. J., Puranen, J. S., Kankaanpää, P., Upla, P., Tulla, M., Johnson, M. S., and Heino, J. (2007) *J. Biol. Chem.* **282,** 14675–14683
30. Tulla, M., Lahti, M., Puranen, J. S., Brandt, A. M., Käpylä, J., Domogatskaya, A., Salminen, T. A., Tryggvason, K., Johnson, M. S., and Heino, J. (2008) *Exp. Cell Res.* **314,** 1734–1743
31. Nykvist, P., Tu, H., Ivaska, J., Käpylä, J., Pihlajaniemi, T., and Heino, J. (2000) *J. Biol. Chem.* **275,** 8255–8261
32. Käpylä, J., Jäälinoja, J., Tulla, M., Ylöstalo, J., Nissinen, L., Viitasalo, T., Vehviläinen, P., Marjomäki, V., Nykvist, P., Säämänen, A. M., Farndale, R. W., Birk, D. E., Ala-Kokko, L., and Heino, J. (2004) *J. Biol. Chem.* **279,** 51677–51687
33. Kabsch, W. (2010) *Acta Crystallogr. D. Biol. Crystallogr.* **66,** 125–132
34. Vagin, A., and Teplyakov, A. (1997) *J. Appl. Crystallogr.* **30,** 1022–1025
35. Collaborative Computational Project No. 4 (1994) *Acta Crystallogr. D Biol. Crystallogr.* **50**, 760–763
36. Murshudov, G. N., Vagin, A. A., and Dodson, E. J. (1997) *Acta Crystallogr. D Biol. Crystallogr.* **53,** 240–255
37. Perrakis, A., Morris, R., and Lamzin, V. S. (1999) *Nat. Struct. Biol.* **6,** 458–463
38. Emsley, P., and Cowtan, K. (2004) *Acta Crystallogr. D Biol. Crystallogr.* **60,** 2126–2132
39. Chen, V. B., Arendall, W.B., 3rd, Headd, J. J., Keedy, D. A., Immormino, R. M., Kapral, G. J., Murray, L. W., Richardson, J. S., and Richardson, D. C. (2010) *Acta Crystallogr. D Biol. Crystallogr.* **66,** 12–21
40. DeLano, W. (2010) *The PyMOL Molecular Graphics System*, version 1.3r1, Schrödinger, LLC, New York
41. Aquilina, A., Korda, M., Bergelson, J. M., Humphries, M. J., Farndale, R. W., and Tuckwell, D. (2002) *Eur. J. Biochem.* **269,** 1136–1144
42. Xiong, J. P., Li, R., Essafi, M., Stehle, T., and Arnaout, M. A. (2000) *J. Biol. Chem.* **275,** 38762–38767
43. Xie, C., Zhu, J., Chen, X., Mi, L., Nishida, N., and Springer, T. A. (2010) *EMBO J.* **29,** 666–679
44. Vorup-Jensen, T., Ostermeier, C., Shimaoka, M., Hommel, U., and Springer, T. A. (2003) *Proc. Natl. Acad. Sci. U.S.A.* **100,** 1873–1878
45. Li, R., Rieu, P., Griffith, D. L., Scott, D., and Arnaout, M. A. (1998) *J. Cell Biol.* **143,** 1523–1534
46. Siljander, P. R., Hamaia, S., Peachey, A. R., Slatter, D. A., Smethurst, P. A., Ouwehand, W. H., Knight, C. G., and Farndale, R.W. (2004) *J. Biol. Chem.* **279,** 47763–47772
47. McCleverty, C. J., and Liddington, R. C. (2003) *Biochem. J.* **372,** 121–127
48. Shimaoka, M., Takagi, J., and Springer, T.A. (2002) *Annu. Rev. Biophys. Biomol. Struct.* **31,** 485–516
49. Shimaoka, M., Shifman, J. M., Jing, H., Takagi, J., Mayo, S. L., and Springer, T. A. (2000) *Nat. Struct. Biol.* **7,** 674–678
50. Jin, M., Andricioaei, I., and Springer, T. A. (2004) *Structure* **12,** 2137–2147
51. Arnaout, M. A., Mahalingam, B., and Xiong J. P. (2005) *Annu. Rev. Cell Dev. Biol.* **21,** 381–410
52. Luo, B. H., Carman, C. V., and Springer, T. A. (2007) *Annu. Rev. Immunol.* **25,** 619–647
53. Moser, M., Legate, K. R., Zent, R., and Fässler, R. (2009) *Science* **324,** 895–899
54. Chen, X., Xie, C., Nishida, N., Li, Z., Walz, T., and Springer, T. A. (2010) *Proc. Natl. Acad. Sci. U.S.A.* **107,** 14727–14732
55. Jokinen, J., White, D. J., Salmela, M., Huhtala, M., Käpylä, J., Sipilä, K., Puranen, J. S., Nissinen, L., Kankaanpää, P., Marjomäki, V., Hyypiä, T., Johnson, M. S., and Heino J. (2010) *EMBO J.* **29,** 196–208
56. Kamata, T., and Takada, Y. (1994) *J. Biol. Chem.* **269,** 26006–26010
57. Morgan, M. R., Humphries, M. J., and Bass, M. D. (2007) *Nat. Rev. Mol. Cell. Biol.* **8,** 957–969
58. Smith, H. W., and Marshall, C. J. (2010) *Nat. Rev. Mol. Cell. Biol.* **11,** 23–36

SUPPLEMENTAL DATA [Lahti et al., (2011)]

Supplementary Figure S1. Expression levels of the mutant α1 integrins were confirmed by flow cytometry. After Zeocin selection positive transfected CHO cells were stained with integrin α_1 antibody (Purified anti-human CD49a, SR-84) and anti-mouse IgG FITC antibody and collected as mixed populations using FACSVantage SE flow cytometry. CHO-cells expressing (A) α1WT (wild-type), (B) α1C139S variant, (C) α1E317A variant, and (D) α1C139S/E317A variant. In all panels non-transfected CHO WT cell represent negative control.